fMRI Study of Sound Pressure Level Encoding in the Different Subdivisions of Inferior Colliculus

Jevin W. Zhang[1,2], Condon Lau[1], Joe S. Cheng[1,2], Iris Y. Zhou[1,2], Matthew M. Cheung[1], and Ed X. Wu[1,2]

[1]*Laboratory of Biomedical Imaging and Signal Processing, The University of Hong Kong, Hong Kong, Hong Kong SAR, China,* [2]*Department of Electrical and Electronic Engineering, The University of Hong Kong, Hong Kong, Hong Kong SAR, China*

Introduction - In all mammals, the inferior colliculus (IC) is the major midbrain nucleus for integration of auditory information from the brainstem. It is composed of a central nucleus (CIC) adjacent to the external cortical nucleus (ECIC) [1]. One important piece of physical auditory information is intensity, which is customarily reported as sound pressure level (SPL) [2]. Intensity is crucial for mediating arousal, emotions, and motivations [3]. The rat IC occupies a larger portion of the brain and is a suitable model for functional imaging. Here we apply non-invasive fMRI with sparse temporal sampling to measure the hemodynamic responses in the rat CIC and ECIC during auditory stimulation at seven SPLs over a 72 dB range. This study can improve our understanding of auditory physiology on SPL encoding.

Methods - *Animal preparation:* Normal male Sprague-Dawley rats (200 – 250g, N=7) were anesthetized with isofluorane (3% for induction and 1% for maintaince). *Animal stimulation:* Monaural broadband noise stimuli were produced by a closed-field electrostatic loudspeaker (TDT EC1) and driven by an amplifier (TDT ED1) and waveform generator (Hewlett-Packard 33120A). Sound was delivered to the left ear canal via a custom built tube. The right ear was occluded with cotton wool and Vaseline. Animals were stimulated using 10s sound off then five paradigms of 10s off and 50s on. During the on periods, the sound was played for 5s every 10s with 4 Hz burst rate and 92% duty cycle (230ms on and 20ms off) (Fig. 1). All of the sound stimuli and fMRI scans were synchronized by triggers sent from a custom designed LabVIEW data control system (NI, Austin, TX). The SPL of the broadband noise during each paradigm was randomly chosen from seven settings (17, 29, 41, 53, 65, 77, and 89 dB). SPL was measured at the end of the tube using an M50 microphone (Earthworks) and a recorder (FR2, Fostex). SPL was varied by adjusting the output voltage of the waveform generator (doubling amplitude increased 6dB) and the gain of the amplifier. The fMRI session was repeated 14 times per animal resulting in ten presentations of each SPL. *MRI protocol:* Experiments were performed on a 7T MRI scanner (PharmaScan, Bruker Biospin GmbH). Thirty one gradient echo echo-planar imaging (GE-EPI) scans (FOV = 32x32 mm^2, data matrix = 64x64, TR = 10.0s, TA = 1.0s, TE = 18ms, 9 slices) were acquired for every session. The 1s acquisition started immediately after the end of each 5 s noise on period and immediately after the 10 s off period at the beginning of a paradigm (Fig. 1). *Data analysis:* The images were realigned first using SPM8 (Wellcome Center, UCL). To identify activated voxels, the sequence of images from a session was split into five blocks, each including one image from immediately after the 10s off period and five images from immediately after each 5s noise on period, for a total of 70 blocks per animal. Blocks corresponding to the same SPL were averaged. Student t-test was performed to identify voxels with statistically significantly positive BOLD signal changes. T-value maps were generated using custom MATLAB code (Mathworks) with the activation threshold set to $t > 7.17$ (equivalent to $p < 0.01$) and cluster size > 3. BOLD signal change maps at seven SPL settings were plotted (Fig. 3). To plot the slope map describing BOLD signal change dependence on SPL (Fig. 2B), linear regression was performed on the signal from each voxel of the seven BOLD signal change maps. The dependence of BOLD signal change on SPL in each structure was determined by linear regression on the average signal within each ROI of the seven BOLD signal change maps (Fig. 4).

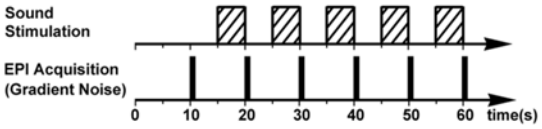

Fig. 1: A schematic representation of the sparse temporal sampling paradigm. Top: The shadows indicate the 5s long broadband noise stimulation. Bottom: The vertical lines indicate acquisition of a single image volume.

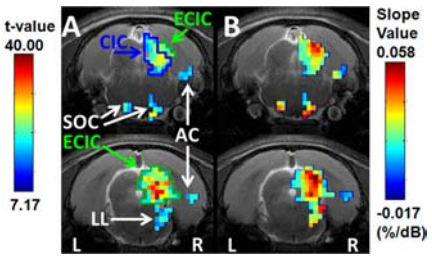

Fig. 2: (A) Functional t-value map from a representative animal computed from the fMRI images. Images acquired at each of the seven SPLs were averaged together. Only voxels with $t > 7.17$, equivalent to $p < 0.01$, and cluster size > 3 are color coded. The color bar on the left indicates the t-value scale. (B) BOLD signal change slope map from the representative animal showing the hemodynamic response's SPL The color bar on the right indicates the slope in units of %/dB.

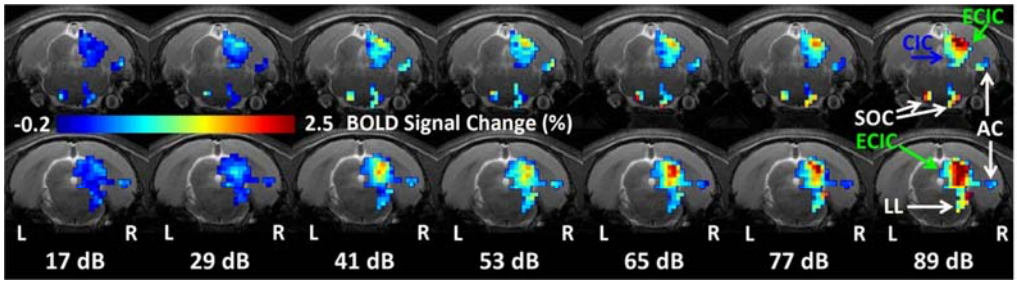

Fig. 3: BOLD signal change map from the representative animal at different SPL settings. The color bar indicates the BOLD signal change scale. Structures are labeled on the 89 dB map. L and R indicate the left and right hemispheres of the brain. Only voxels with $t > 7.17$ and cluster size > 3 in the activation map are color coded (refer to Fig. 2A).

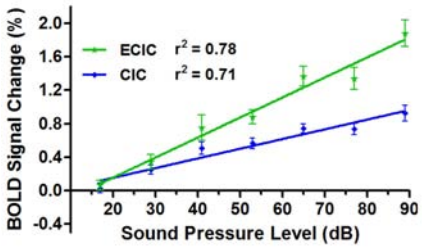

Fig 4: BOLD signal change (mean ± standard error of mean) vs. SPL and the best-fit linear regression lines obtained using the least squares approach. r^2 is the square of the Pearson product-moment correlation coefficient and describes goodness of fit.

Results - Fig. 2A shows the t-value map from a representative animal. The BOLD signal change slope map from the animal is shown in Fig. 2B. The slope map plots the hemodynamic response amplitude's SPL dependence. Almost all voxels have positive slope. Voxels with highest slopes appear in the ECIC. In lateral lemniscus, the voxels in the dorsal nucleus appear to have higher slopes than those in the ventral nucleus. In superior olivary complexe, the slope is also large. Voxels in auditory cortex have lowest slopes. The dependence of BOLD signal change on SPL is also demonstrated in Fig. 3, which shows the BOLD signal change map from the same animal at each SPL setting. To further compare the hemodynamic response SPL dependences in different subdivisions, the BOLD signal changes from all voxels in each ROI were averaged and compared. Functionally defined CIC and ECIC ROIs used in computing the BOLD signal changes are delineated using the t-value map in Fig. 2A. The mean and standard deviation of the number of voxels in each ROI is 25.6 ± 3.9 (CIC), 41.1 ± 8.6 (ECIC) cross the seven animals. Fig. 4 shows the BOLD signal change (mean ± standard error of mean) vs. SPL and the linear regression lines for the CIC and ECIC ROIs. The Pearson correlation coefficient values (r^2) for the CIC, ECIC are 0.71, 0.78 respectively which shows that their responses are close to linear. The slope of ECIC (0.024 %/dB) is significantly larger than that of CIC (0.012 %/dB) ($p < 0.001$).

Discussion - In the IC, Aitikin et al., Palombi et al., and Syka et al. have all reported that the ECIC has a higher percentage of monotonic neurons than the CIC [4-6]. Therefore, the mean rate-intensity function in the ECIC is more monotonic [7]. These findings are in good agreement with our fMRI data from the CIC and ECIC in Figs. 2 to 4 because fMRI BOLD signals are highly correlated with neuronal firing rate [8-10]. From our results, the BOLD signal changes increase with SPL in both the ECIC and CIC, but the slope in the ECIC is significantly higher than that in the CIC ($p < 0.001$), possibly due to a greater fraction of monotonic neurons in the ECIC. Further, the SPL dependence measured in this study is very similar to that measured in our earlier study using the continuous imaging method [11]. Therefore, sparse temporal sampling may not be a prerequisite in auditory fMRI studies of the IC.

References - [1] Winter, J.A. The IC, 2005; [2] Pierce, A.D., Acoustics, [3] Bradley, M.M., Psychophysiol; [4] Palombi, P.S., J Neurophysiol; [5] Syka, J., Exp Brain Res, 2000; [6] Aitkin, L., Exp Brain Res, 1994; [7] Palombi, P.S., Hearing Res, 1996; [8] Hyder, F., PNAS, 2002; [9] Logothetis, N.K., Annual Review of Physiol, 2002; [10] Mukamel, R., Science, 2005; [11] Cheung M.M., Neuroimage, 2012.